Atherosclerosis 242 (2015) 251–260

Contents lists available at ScienceDirect

Atherosclerosis

journal homepage: www.elsevier.com/locate/atherosclerosis

Valvular interstitial cells suppress calcification of valvular endothelial cells

Jesper Hjortnaes [a, d, 1], Kayle Shapero [b, 1], Claudia Goettsch [c], Joshua D. Hutcheson [c], Joshua Keegan [a], Jolanda Kluin [d], John E. Mayer [e], Joyce Bischoff [b], Elena Aikawa [a, c, *]

[a] Center of Excellence in Vascular Biology, Cardiovascular Medicine, Brigham and Women's Hospital, Harvard Medical School, Boston, United States
[b] Vascular Biology Program and Department of Surgery, Boston Children's Hospital, Harvard Medical School, Boston, United States
[c] Center for Interdisciplinary Cardiovascular Sciences, Brigham and Women's Hospital, Harvard Medical School, Boston, United States
[d] Department of Cardiothoracic Surgery, University Medical Center Utrecht, Utrecht, The Netherlands
[e] Department of Thoracic Surgery, Boston Children's Hospital, Harvard Medical School, Boston, United States

ARTICLE INFO

Article history:
Received 29 March 2015
Received in revised form
2 July 2015
Accepted 2 July 2015
Available online 17 July 2015

Keywords:
Calcific aortic valve disease
Valvular endothelial cells
Valvular interstitial cells
Calcification
Endothelial-to-mesenchymal transformation

ABSTRACT

Background: Calcific aortic valve disease (CAVD) is the most common heart valve disease in the Western world. We previously proposed that valvular endothelial cells (VECs) replenish injured adult valve leaflets via endothelial-to-mesenchymal transformation (EndMT); however, whether EndMT contributes to valvular calcification is unknown. We hypothesized that aortic VECs undergo osteogenic differentiation via an EndMT process that can be inhibited by valvular interstitial cells (VICs).

Approach and results: VEC clones underwent TGF-β_1-mediated EndMT, shown by significantly increased mRNA expression of the EndMT markers α-SMA (5.3 ± 1.2), MMP-2 (13.5 ± 0.6) and Slug (12 ± 2.1) ($p < 0.05$), (compared to unstimulated controls). To study the effects of VIC on VEC EndMT, clonal populations of VICs were derived from the same valve leaflets, placed in co-culture with VECs, and grown in control/TGF-β_1 supplemented media. In the presence of VICs, EndMT was inhibited, shown by decreased mRNA expression of α-SMA (0.1 ± 0.5), MMP-2 (0.1 ± 0.1), and Slug (0.2 ± 0.2) ($p < 0.05$). When cultured in osteogenic media, VECs demonstrated osteogenic changes confirmed by increase in mRNA expression of osteocalcin (8.6 ± 1.3), osteopontin (3.7 ± 0.3), and Runx2 (5.5 ± 1.5). The VIC presence inhibited VEC osteogenesis, demonstrated by decreased expression of osteocalcin (0.4 ± 0.1) and osteopontin (0.2 ± 0.1) ($p < 0.05$). Time course analysis suggested that EndMT precedes osteogenesis, shown by an initial increase of α-SMA and MMP-2 (day 7), followed by an increase of osteopontin and osteocalcin (day 14).

Conclusions: The data indicate that EndMT may precede VEC osteogenesis. This study shows that VICs inhibit VEC EndMT and osteogenesis, indicating the importance of VEC–VIC interactions in valve homeostasis.

1. Introduction

Calcific aortic valve disease (CAVD) and subsequent aortic valve stenosis is the most common heart valve disease in the Western world [1,2]. CAVD is currently considered an actively regulated and progressive disease, characterized by a cascade of cellular changes that initially cause fibrotic thickening, followed by extensive calcification of the aortic valve leaflets. This in turn leads to significant aortic valve stenosis and eventual left ventricular outflow obstruction [3,4], for which surgical replacement remains the only viable treatment option.

Heart valves contain a heterogeneous population of valvular

Abbreviations: CAVD, calcific aortic valve disease; VEC, valvular endothelial cell; EndMT, endothelial-to-mesenchymal transformation; VIC, valvular interstitial cell; α-SMA, alpha-smooth muscle actin; MMP-2, matrix metalloproteinase 2; TGF-β_1, transforming growth factor beta 1; qVICs, quiescent fibroblast-like VIC; aVICs, activated myofibroblast-like VICs; oVICs, osteoblast-like VICs; EBM-2, endothelial basal media; FBS, fetal bovine serum; GPS, glutamine-penicillin-streptomycin; bFGF, basic fibroblast growth factor; DMEM, Dulbecco's modified eagles media; OM, osteogenic media; NM, control media; PBS, phosphate buffered saline; PFA, paraformaldehyde; NBT/BCIP, nitro-blue tetrazolium/indolylphosphate; ALP, alkaline phosphatase.

* Corresponding author. Cardiovascular Medicine, Brigham and Women's Hospital, 77 Ave Louis Pasteur, NRB-741, Boston, MA 02115, United States.
E-mail address: eaikawa@partners.org (E. Aikawa).

[1] Equal contribution.

http://dx.doi.org/10.1016/j.atherosclerosis.2015.07.008

endothelial cells (VECs) and valvular interstitial cells (VICs), which maintain valve homeostasis and structural leaflet integrity. VICs, the most abundant cell type in the heart valve, play a key role in CAVD progression. Various VIC phenotypes have been identified in diseased human heart valves [5], including quiescent fibroblast-like VICs (qVICs), which upon pathological cues can differentiate into activated myofibroblast-like VICs (aVICs); and osteoblast-like VICs (oVICs), which are responsible for the active deposition of calcium in CAVD [6–8]. Additionally, numerous studies have demonstrated the ability of VICs to undergo osteogenic differentiation [9–11]. Relatively little is known about the role of VECs in CAVD. VECs cover the surface of the heart valve to form an endothelial monolayer, and are unique in that they can undergo endothelial-to-mesenchymal transformation (EndMT) — a critical process in developmental valvulogenesis [12–15]. During development, EndMT occurs in the endocardial cushions, where a subset of endothelial cells detach from the endothelium, transiently enhance the contractile protein α-SMA, and migrate into the interstitium of the embryonic valve to become VICs [13,16,17]. EndMT also occurs in adult valves, where cells co-expressing endothelial markers and α-SMA have been detected along the valve endothelium and in subendothelial locations [18]. These observations prompted the hypothesis that low or basal levels of EndMT contribute to the replenishment of VICs as part of physiologic valve remodeling that is required throughout postnatal life [19]. We recently demonstrated that EndMT plays a role in the adaptive pathologic remodeling of mitral valve leaflets in an ovine model of functional mitral regurgitation [20,21]. In addition, EndMT has shown to be potentiated by exposure to cyclic mechanical strain [22]. We furthermore showed that mitral VECs are able to differentiate *in vitro* into mesenchymal lineages, including osteogenic cells [14].

VECs have been indicated as key regulators in early CAVD via recruitment of immune cells [23], dysregulation of protective nitric oxide (NO) signaling [24,25], and phenotypic plasticity through the expression of procalcific proteins [14]. Collectively, these studies indicate a potential role for dysregulated VECs in valvular disease, but the role of EndMT in aortic valve leaflet calcification in CAVD is yet unknown. Furthermore, factors that regulate EndMT-associated VEC differentiation into osteogenic cells remain unclear. Based on our previous investigations, we hypothesized that VEC–VIC interaction serves as a native barrier to prevent excessive VEC EndMT and subsequent osteogenic differentiation.

2. Methods

2.1. Aortic valve cell isolation

Ovine tissues from animals 8–10 months of age, weighing 20–25 kg, were obtained under approved NIH guidelines for animal experimentation as performed at Children's Hospital Boston. Valve leaflets were incubated in endothelial basal medium (EBM-2) (CC- 3156, Cambrex Bio Science, Walkersville, MD) with 5% fetal bovine serum (FBS) (Hyclone, Logan, UT), 1% GPS (Invitrogen, Carlsbad, California), 2 mmol/L L-glutamine, and 100 μg/ml gentamicin sulfate for 1–4 h. They were then minced into 2-mm pieces and incubated with 0.2% collagenase A (Roche Diagnostics, Indianapolis, IN) in EBM-2 for 5 min at 37 °C, and diluted with Hanks' balanced salt solution containing 5% FBS, 1.26 mmol/L $CaCl_2$, 0.8 mmol/L $MgSO_4$, and 1% GPS (wash buffer). The supernatant was sedimented at 200 × g, resuspended in VEC medium (EBM-2 medium, 10% heat-inactivated FBS, 1% GPS, and 2 ng/mL basic fibroblast growth factor [bFGF]; Roche Diagnostics, Indianapolis, IN) and plated. The following day, primary cultures were washed to remove unattached cells. Primary cultures were trypsinized, resuspended in growth medium at 3.3 cells/ml, and 100 μl were plated in each well of a 96-well plate, at a concentration of approximately one cell to every third well; visual inspection was performed to assess that single colonies appeared in a subset of wells. When the colonies covered two-thirds of the well, cells were split into 24-well dishes. Based on morphology, these clones were initially visually identified as either endothelial or interstitial. These observations were confirmed with phenotypic characterization and designated as either endothelial (VEC) [26,27] or interstitial (VIC-K3, VIC-K5, VIC-K6), and expanded on 1% gelatin-coated dishes in VEC media. Cells were passaged 1:3 or 1:4 every 6–14 days, and experiments were performed using VEC and VIC clones between passages 8 and 14. VECs were grown in VEC media, and VICs were cultured in VIC media (DMEM, 10% FBS, 1% GPS).

2.2. Human calcified aortic valves

Aortic valve leaflets (n = 5) were harvested from patients undergoing aortic valve replacement for aortic valve stenosis and a healthy valve was obtained from autopsy, performed using criteria established by the declaration of Helsinki. Tissue samples were frozen in optimal cutting temperature compound (OCT, Sakura Finetech, Torrance, CA) and 7 μm serial sections were cut and stained. Tissue was collected according to Brigham and Women's Hospital IRB Protocols.

2.3. Mouse model of CAVD

Male apolipoprotein E-deficient mice ($apoE^{-/-}$ mice; 10 weeks old) were purchased from Jackson Laboratory (Bar Harbor, ME). High-fat diet (21% fat and 0.21% cholesterol) was obtained from Research Diets (D12079B, New Brunswick, NJ). Mice were fed with an atherogenic diet for a total of 22 weeks. Mice were euthanized for tissue collection and histopathology at 32 weeks. The animal procedures were performed conform the NIH guidelines and approved by the Brigham and Women's Hospital Animal Care and Use Committee. This model is characterized by the presence of functional and histopathological changes found in human CAVD [33].

2.4. Endothelial-to-mesenchymal transformation (EndMT)

EndMT was induced as described previously [27]. The assay was also performed in the presence of VICs in an indirect co-culture system, using a Transwell system (12-mm Transwells with 0.4-μm pore polycarbonate membrane inserts; Corning Life Sciences, Acton, MA) (Supplemental Fig. I). Briefly, VECs were grown alone or in co-culture with VICs in VEC media, or VEC media supplemented with 2 ng/mL TGF-β_1 (R&D Systems, Minneapolis, MN), for up to 14 days. Media was changed every 2–3 days.

2.5. VEC and VIC osteogenic potential

The osteogenic potential of VEC and VIC clones was tested both separately and in co-culture for up to 21 days via treatment with osteogenic media (OM) (DMEM with 10% FBS, 1% GPS with 10 nmol/L beta-glycerolphosphate, 50 μmol/L ascorbic acid, 10 μmol/L dexamethasone). DMEM with 10% FBS, 1% GPS was used as control medium (NM). Media was changed every 2–3 days.

2.6. VEC-VIC indirect co-culture

Co-culture experiments were performed using Transwell plates (Corning, Tewksbury, MA) (Supplemental Fig. I). Cells were plated either in the Transwell inserts or on the bottom of 6-well plates at a density of 1×10^5 cells/cm^2 and allowed to adhere overnight. After

24 h, the two cell types were combined to begin the co-culture by placing the inserts into the corresponding well of the 6 well plate. For the conditioned media experiments, cells were treated with media that had been conditioned by the specific cell type for 24 h. Conditioned media was sterile-filtered and added in a 1:1 ratio with fresh media to treated cells. Media was changed every 2–3 days.

2.7. Histological detection of VEC and VIC mineralization

Upon completion of experiments, cells were washed with PBS and fixed using 4% paraformaldehyde for 15 min. Cells were subsequently washed with PBS. Mineralization was analyzed by staining with 0.02 mg/L of Alizarin Red S (Sigma–Aldrich). The area of positive Alizarin Red S staining was normalized to cell number. To detect the expression of alkaline phosphatase (ALP), nitro-blue tetrazolium/indolylphosphate (NBT/BCIP) staining was performed. Before staining, the cells were washed with PBS, 0.5 ml of NBT/BCIP was added, and the samples were then incubated at 37 °C in a humidified chamber containing 5% CO_2 for 30 min. Samples were then washed with PBS and fixed with 4% PFA, after which they underwent a counter stain with 0.1% eosin for 5 min. Images were taken with an Eclipse 80i microscope (Nikon) and processed with Elements 3.20 software (Nikon).

2.8. Alkaline phosphatase activity and calcium measurements

A colorimetric kit was used to measure ALP activity (BioVision, Milpitas, CA) according to the manufacturer's instructions. 16 μl of supernatant from 12-well plates was added to 64 μl of ALP assay buffer and 50 μl of PnPP solution was added and incubated for 1 h at room temperature. The absorbance was read at a wavelength of 405 nm. Values were normalized to the standard curve. Calcium content was quantified using a colorimetric kit (BioVision) according to the manufacturer's protocol. Briefly, 50 μL of sample was added to 60 μL of calcium assay buffer, after which 90 μL of chromogenic reagent was added and incubated for 10 min at room temperature in the dark. Absorbance was read at a wavelength of 575 nm with a plate reader. Values were normalized to the standard curve.

2.9. Immunofluorescence and western blotting

Immunofluorescence staining was performed on methanol-fixed cells and human and mouse aortic valve leaflets using anti-human VE-cadherin (Santa Cruz) or CD31 (Cell Signaling), anti-human α-SMA (clone 1A4, Sigma–Aldrich), anti-vimentin antibody (Abcam, Cambridge, MA) and anti-osteocalcin (Abcam). Secondary antibodies conjugated with AlexaFluor 488 (Invitrogen) were used. Images were taken with an Eclipse 80i microscope (Nikon) and processed with Elements 3.20 software (Nikon). For western blotting, cells were lysed as previously described [14]. Briefly, cells were lysed with 4 mol/L urea, 0.5% SDS, 0.5% NP-40, 100 mmol/L Tris, and 5 mmol/L EDTA, pH 7.4, containing 100 μmol/L leupeptin 10 mmol/L benazmidine, 1 mmol/L PMSF, and 12.5 μg/mL aprotinin. Lysates were subjected to 10% SDS-PAGE (13 μg of protein per lane) and transferred to Immobilon-P membrane (Millipore, Bedford, MA). Membranes were incubated with murine anti-human α-SMA, goat anti-human CD31, and goat anti-human VE-Cadherin diluted in 5% dry milk in 1x PBS-T (0.1% Tween-20, 25 μM Tris-HCL, 0.15 M NaCl in PBS), and then with secondary antibody (peroxidase-conjugated anti-mouse or anti-goat). Antigen–Ab complexes were visualized using chemiluminescent sensitive film. Equal protein amounts (12–15 μg) were loaded in each lane (determined by u-BCA assay, Pierce), and expression was quantified via densitometry analysis and normalized to that of β-actin (Sigma). All antibodies were shown to cross-react with their ovine homologs.

2.10. Real-time polymerase chain reaction

Total RNA was isolated using RNeasy Mini Kit (Qiagen), supplemented with DNase I treatment (Qiagen). Reverse transcription was performed with Superscript II cDNA synthesis kit (Invitrogen/Life Technologies, Grand Island, NY) to obtain a target cDNA concentration of 0.335 μg/mL, followed by RT-PCR using SYBR Green (BioRad, Hercules, CA), and annealing temperatures of 95 °C and 60 °C for 35 cycles. Oligonucleotide primer sequences are presented in Supplementary Table 1. All PCR products were sequenced using ABi DNA sequences (Children's Hospital Boston core facility) to verify the sequence corresponding to the gene of interest (Supplementary Table 1).

2.11. Migration assay

100 μg/mL rat tail collagen type I (0.02 N acetic acid) was used to coat 6.5-mm Transwells with 8.0-μm pore polycarbonate membrane inserts for 1 h at 37 °C, followed by one wash with PBS. Cells were treated as specified, trypsinized, and seeded in the upper chamber of the transwell plate at a density of 1×10^4 cells/well (100 μl volume). 300 μL of control media (EBM-2/serum-free and growth factor-free) or VEC media supplemented with 20% FBS was added to the lower chamber. Cells were then allowed to migrate for 4 h at 37 °C. The cells in the upper chamber were gently removed using a cotton swab, and the lower surface was fixed with ice-cold methanol and mounted on glass slides in mounting media containing DAPI. Cells were counted using a fluorescent microscope.

2.12. Statistical analysis

Results are presented as mean ± standard deviation (SD) unless indicated otherwise. Unpaired Student's t-test was used for comparisons between two groups. One-way ANOVA was used to evaluate statistical significant differences in multiple groups. $P < 0.05$ was considered statistically significant.

3. Results

3.1. TGF-β1 and osteogenic media induce VEC EndMT

Clonal populations from ovine aortic valve leaflets were isolated using a brief collagenase-A procedure, which has been described previously [12]. The VEC clone demonstrated cobblestone endothelial morphology and stained positively for VE-Cadherin and negatively for α-SMA (Supplementary Fig. II). VIC clonal populations from the same valve were isolated and characterized. Immunofluorescence staining of the aortic VIC clones (VIC-K3, VIC-K5, and VIC-K6) confirmed the characteristic myofibroblastic phenotype of VICs grown in culture, with positive staining for α-SMA and vimentin and negative staining for the endothelial cell marker VE-Cadherin (Supplementary Fig. III).

In accordance with our earlier work [12], this VEC clone was able to undergo TGF-β_1-induced EndMT, as visualized by anti-α-SMA immunofluorescence after 8 days of TGF-β_1 stimulation (Supplementary Fig. IVA). Western blot analysis confirmed the changes in protein expression (Supplemental Fig. IVB). Significant increases in mRNA expression of the EndMT markers α-SMA (5.3 ± 1.2), MMP-2 (13.5 ± 0.6) and Slug (12 ± 2.1), as well as a decrease of the endothelial marker VE-Cadherin (0.2 ± 0.1) ($p < 0.05$) confirmed TGF-β_1-induced EndMT of the VECs ($n = 3$,

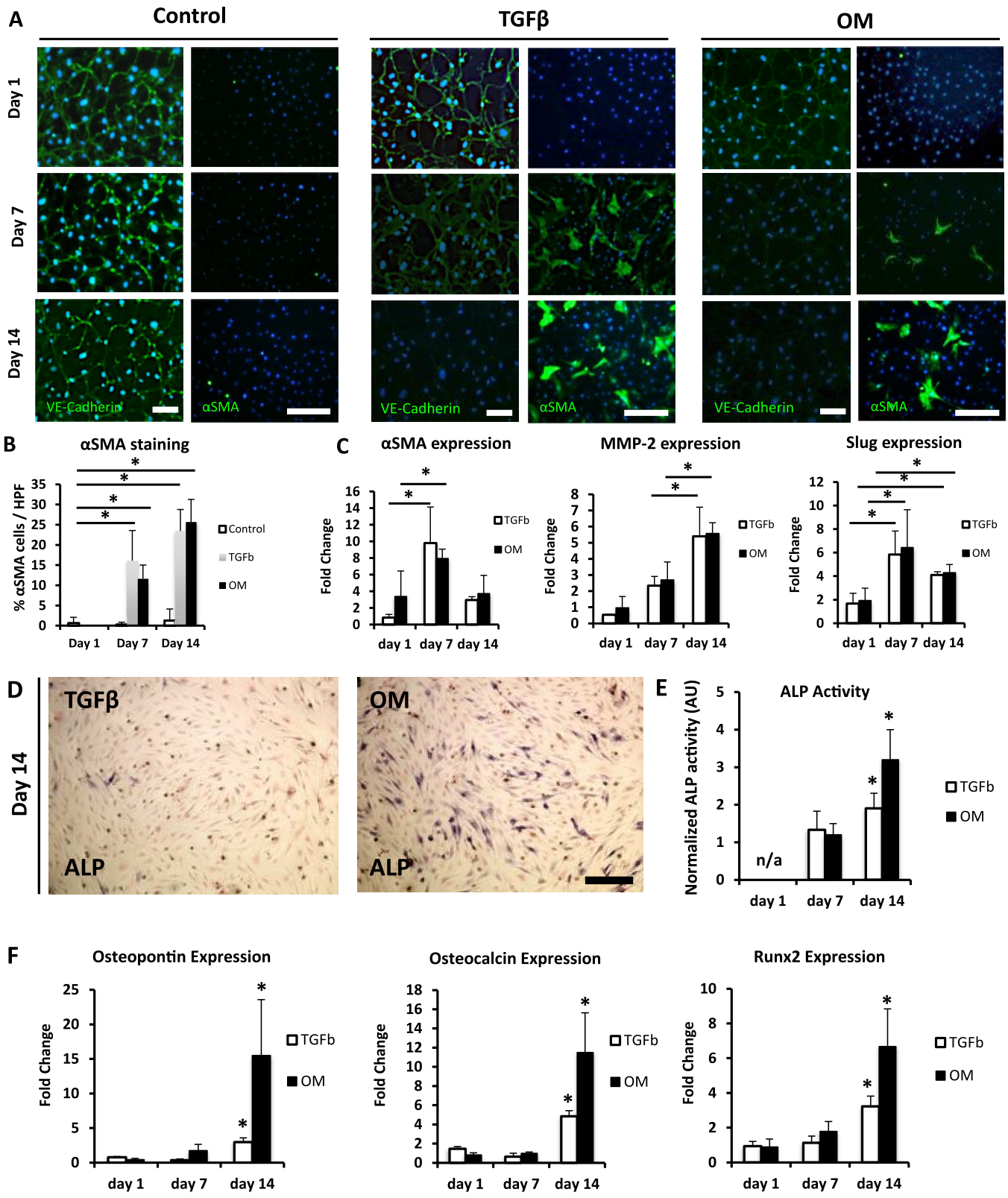

Fig. 1. A–C. EndMT may precede VEC osteoblastic differentiation. VECs (n = 3) were treated with normal media (NM) or osteogenic media (OM) ± TGF-β_1 for 1, 7 or 14 days. A: Immunofluorescence staining of VE-cadherin and α-SMA (green), cell nuclei (DAPI/blue). (n = 3). Bar = 50 μm. B: Quantification of α-SMA staining. C: mRNA expression of α-SMA, MMP-2 and Slug. Data is depicted as mean ± SD fold change, *p < 0.05. D: ALP staining of VECs in media + TGF-β_1 or OM at day 14. (n = 3). Bar = 50 μm. E: ALP activity of VECs in media + TGF-β_1 or OM. Data is depicted as mean ± SD/normalized to NM conditions, *p < 0.05. F: mRNA expression of osteopontin, osteocalcin and Runx2. Data is depicted as mean ± SD fold change, *p < 0.05.

Supplementary Fig. IVC–F).

We performed a time-course analysis of EndMT-associated proteins in VECs treated with either TGF-β_1 or osteogenic media (OM) for up to 14 days. VECs were stained for VE-cadherin and α-SMA at days 1, 7, and 14 of culture (Fig. 1A). Both TGF-β_1 and OM induced a progressive loss of VE-cadherin compared to NM in the VECs. Quantification of α-SMA-positive cells confirmed the increase of myofibroblast-like differentiation of VECs after day 7 and day 14, as compared to day 1 ($p < 0.05$). When VECs were cultured in OM, a higher percentage of α-SMA-positive cells were present on day 14, as compared to day 7 (Fig. 1B). RT-PCR analysis of EndMT markers revealed a significant increase in mRNA expression of α-SMA at day 7 relative to day 1 when cultured with TGF-β_1 (9.8 ± 4.3) and OM (7.9 ± 1.1), but α-SMA expression decreased at day 14 as compared to day 7 (Fig. 1C). In cells stimulated with TGF-β_1 or OM, MMP-2 expression increased significantly from day 7 (TGF-β_1: 2.3 ± 0.5; OM: 2.7 ± 1.1) to day 14 (TGF-β_1: 5.4 ± 1.8; OM: 5.6 ± 0.7). Slug expression follows a similar pattern to α-SMA, demonstrating a significant increase at day 7 (TGF-β_1: 5.8 ± 1.9; OM: 6.4 ± 2.2) compared to day 1 ($p < 0.05$). While day 14 for Slug was not significantly different from day 7, it remained significantly increased as compared to day 1 (TGF-β_1: 4.1 ± 0.3; OM: 2.6 ± 0.7) (Fig. 1C). The increase in expression of these EndMT markers between days 1 and 7 suggests that a process of EndMT occurs in both the VECs treated with TGF-β_1 and those treated with OM.

3.2. Osteogenic differentiation follows EndMT in VECs

We next evaluated osteogenic differentiation over time. We detected a small number of ALP-positive cells following 14 days of stimulation with TGF-β_1, but when VECs were cultured in OM, a more pronounced ALP staining was observed (Fig. 1D). This observation was confirmed by quantification of the ALP activity (OM: 3.2 ± 0.8 vs. TGF-β_1: 1.9 ± 0.4 (Fig. 1E). TGF-β_1 significantly increased osteopontin (2.9 ± 0.6) osteocalcin (4.8 ± 0.5), and Runx2 (3.2 ± 0.5) mRNA expression ($p < 0.05$) at day 14 (Fig. 1F). In addition, when we cultured VECs in OM, we found a significant increase in osteopontin (15.5 ± 8.1), osteocalcin (11.5 ± 4.3), and Runx2 (6.7 ± 2.1) expression at day 14, as compared with earlier time points ($p < 0.05$) (Fig. 1F).

3.3. VICs suppress TGFβ$_1$-induced EndMT of VECs

The presence of VICs (in co-culture) attenuated TGF-β_1-induced EndMT. VICs suppressed TGF-β_1-induced expression of α-SMA in VECs, as demonstrated by immunofluorescence staining (Fig. 2A) and confirmed by Western blot. Three different VIC clones suppressed the EndMT marker α-SMA when the VECs were stimulated with TGF-β_1 (Fig. 2B, Supplementary Fig. V). VICs significantly suppressed the expression of three EndMT markers in TGF-β1 treated VECs: α-SMA (0.1 ± 0.5), MMP-2 (0.1 ± 0.1) and Slug (0.2 ± 0.2) (three different VIC clones, $p < 0.05$; Fig. 2C–E). A similar inhibition of EndMT markers was observed when using VIC conditioned media at a 1:1 ratio (Supplementary Fig. VI). The presence of VICs also inhibited TGF-β_1-induced migration potential of VECs that were first co-cultured with VICs and TGF-β_1, as compared to VECs treated with TGF-β_1 alone (Supplementary Fig. VII).

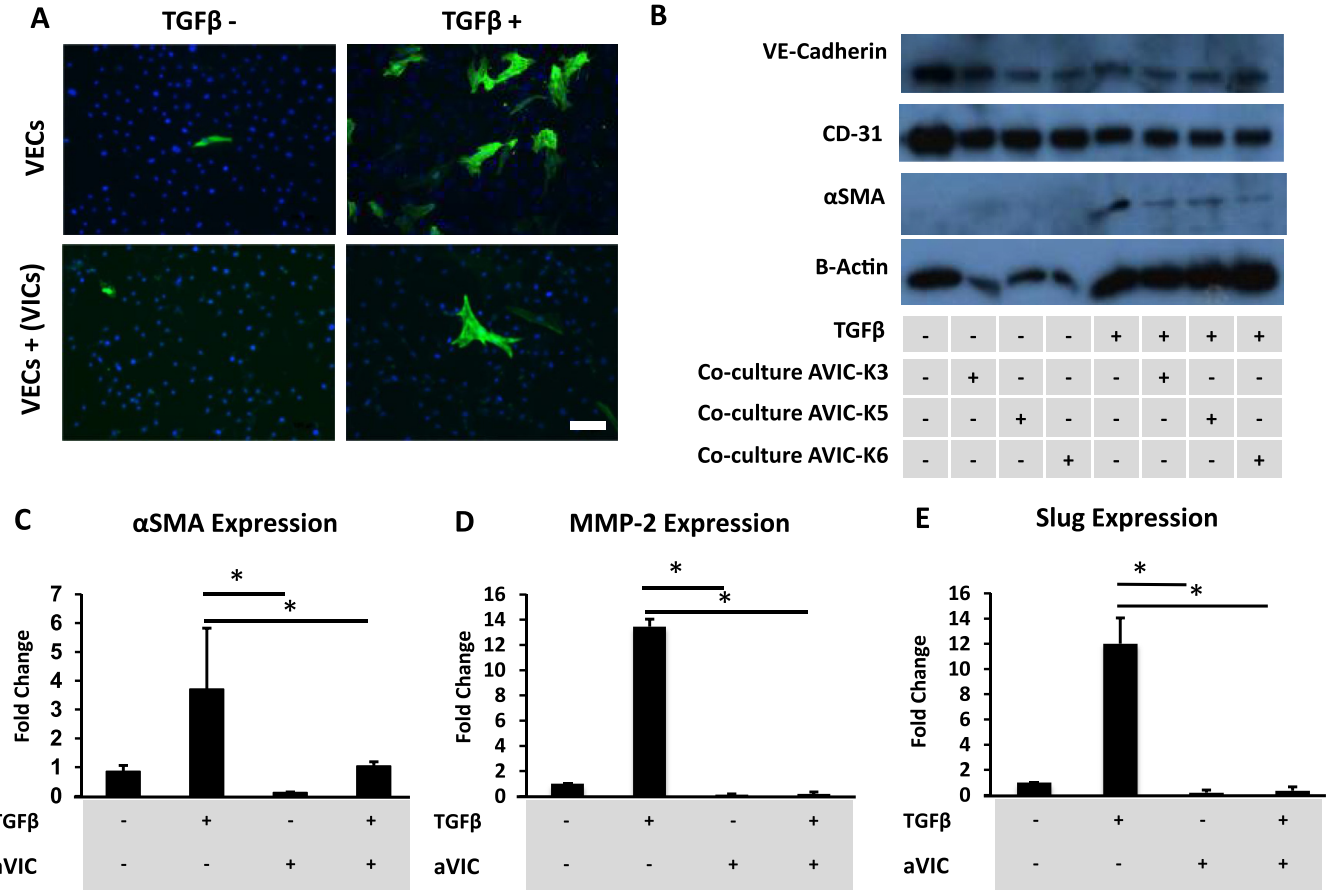

Fig. 2. VICs suppress TGF-β_1-induced VEC EndMT. VECs (n = 3) were co-cultured with VICs (n = 3) in a Transwell culture system and treated with TGF-β_1 for 8 days. A: Immunofluorescence staining of α-SMA (green), cell nuclei (DAPI/blue). (n = 3). Bar = 50 μm. B: Western blot for endothelial markers (VE-cadherin, CD31) and myofibroblastic marker (α-SMA). C: mRNA expression of EndMT markers α-SMA, MMP-2 and Slug. Data is depicted as mean ± SD fold change, *$p < 0.05$.

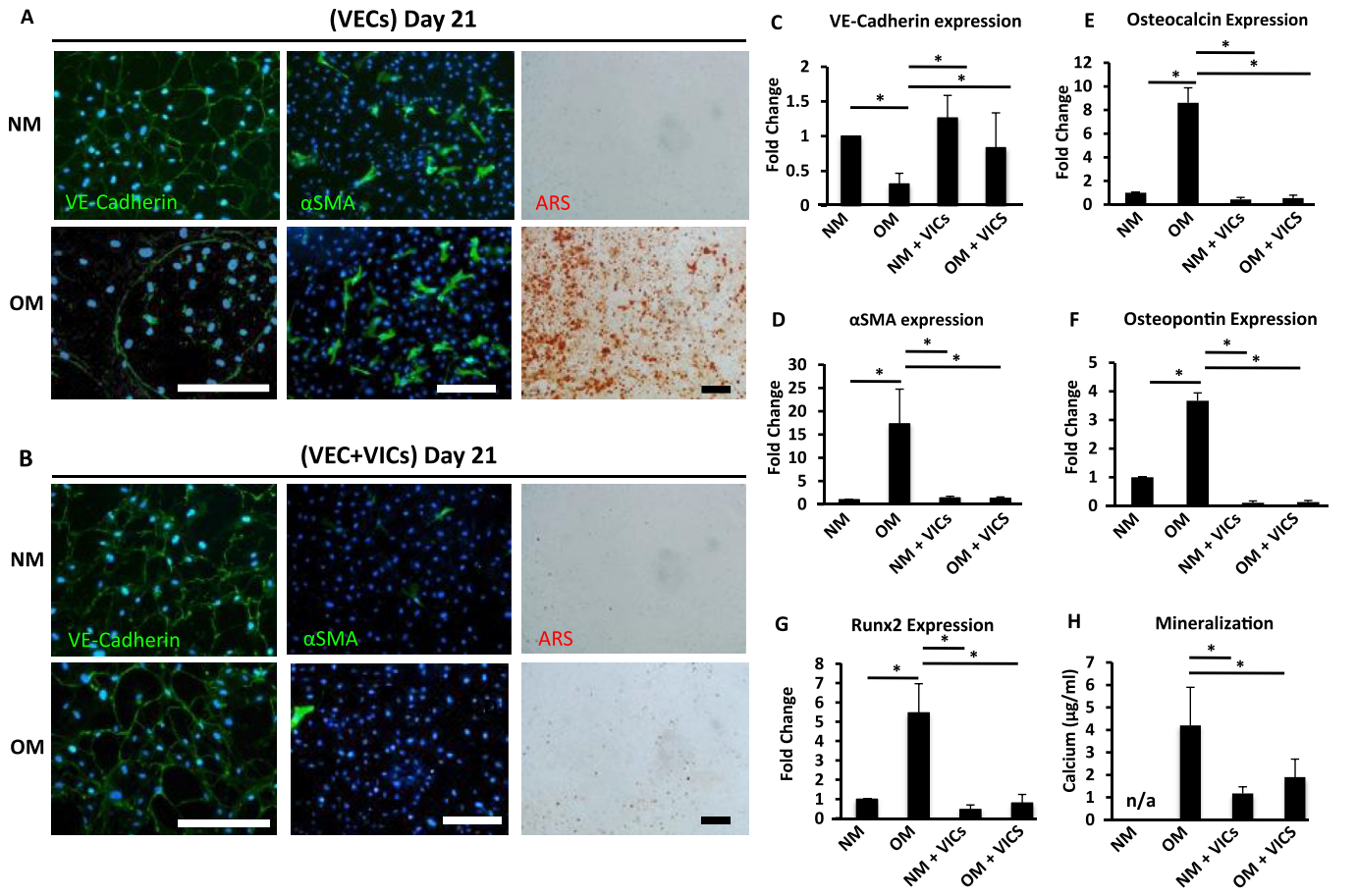

Fig. 3. VICs suppress OM-induced VEC osteogenesis. VECs were co-cultured with VICs in a Transwell culture system in osteogenic media (OM) for 21 days. A–B: Immunofluorescence staining of VE-cadherin (green), α–SMA (green), cell nuclei (DAPI/blue), and Alizarin Red S (ARS) (red/orange). (n = 3). Bar = 50 μm. C: mRNA expression of VE-cadherin, D: α-SMA, E: Osteocalcin, F: Osteopontin, G: Runx2. H: Calcium content. Data is depicted as mean ± SD fold change, *p < 0.05.

3.4. VICs inhibit osteogenic differentiation of VECs

VECs were cultured in OM to evaluate their osteogenic differentiation capacity, using DMEM-based normal growth media (NM) as a control. VECs cultured in OM for 21 days demonstrated a loss of VE-Cadherin, compared with VECs cultured in NM (Fig. 3A). Mineralized matrix, visualized using Alizarin Red S staining, was observed after culturing VECs for 21 days in OM, but was not detected in VECs cultured in NM (Fig. 3A). The presence of VICs (in co-culture) prevented both the OM-mediated decrease in VE-Cadherin and the increase in mineralized matrix (Fig. 3B). There was no difference in cell number between groups (Supplementary Fig. VIII). Analyses of mRNA expression at day 21 confirmed the inhibitory effect of VICs on the osteogenic differentiation of VECs. VE-Cadherin expression decreased significantly in VECs in OM compared to NM (0.3 ± 0.2 $p < 0.05$). This decrease was inhibited by the presence of VICs in co-culture (0.8 ± 0.5) (Fig. 3C). Expression of α-SMA increased when VECs were cultured in OM (17.3 ± 7.5, $p < 0.05$), and this increase was mitigated by the presence of VICs in co-culture (1.3 ± 0.7) (Fig. 3D). VEC cultured in OM showed increased expression of osteocalcin (8.6 ± 1.3, $p < 0.05$), osteopontin (3.7 ± 0.3, $p < 0.05$) and Runx2 (5.5 ± 1.5, $p < 0.05$), compared with cells cultured in NM (Fig. 3E–G). The co-culture of VECs with VICs in OM abolished the induction of osteogenic differentiation markers. A functional consequence of osteogenic differentiation, calcium deposition, increased when VECs were cultured in OM alone, but was significantly impaired when VECs were co-cultured with VICs (OM: 4.2 ± 1.7 μg/mL, OM + VICs: 1.9 ± 0.8 μg/mL, $n = 3$, $p < 0.05$) (Fig. 3H).

3.5. VECs do not suppress osteogenic differentiation of VICs

We evaluated whether VECs have a similar inhibitory effect on the osteogenic differentiation of VICs. VICs cultured in OM for 21 days demonstrated mineralized matrix by Alizarin Red S staining (Fig. 4A). When VICs were co-cultured with VECs in NM or OM, VICs also stained positively for both α-SMA and calcium (Fig. 4B). Expression of α-SMA increased in VICs cultured for 21 days in OM (1.4 ± 0.3, $p < 0.05$) (Fig. 4C). VICs cultured in OM with VECs demonstrated a significant decrease in α-SMA expression (0.2 ± 0.1 $p < 0.05$). The mRNA expression of osteogenic differentiation markers osteocalcin, osteopontin, and Runx2 and the activity of ALP further revealed that VECs do not exhibit an inhibitory effect on VIC osteogenic differentiation (Fig. 4D–F, Supplementary Fig. IX). Functionally, we observed a significant increase in VIC calcium deposition in the co-culture samples (Fig. 4G).

3.6. Human and mouse calcified aortic valves leaflets demonstrate EndMT

After observing EndMT in isolated aortic VECs, we evaluated the presence of EndMT in human calcified aortic valve leaflets. Using immunofluorescence we demonstrate co-expression of α-SMA and CD31 (Fig. 5), confirming the presence of EndMT in calcific valves.

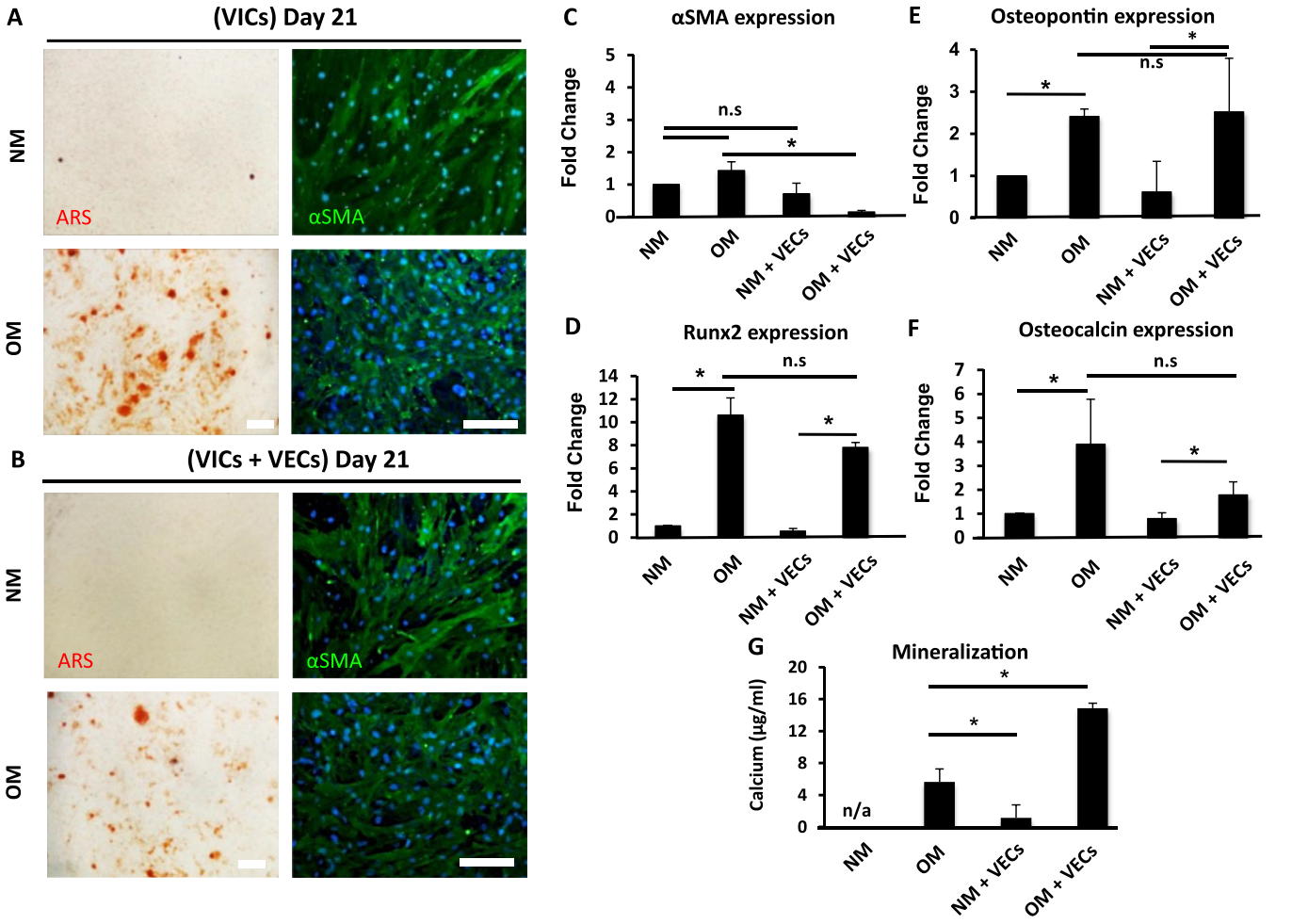

Fig. 4. VECs do not suppress OM-induced VIC osteogenesis. VICs (n = 3) were co-cultured with VECs in a Transwell culture system in osteogenic media (OM) for 21 days. A–B: Immunofluorescence staining of Alizarin Red S (ARS, red/orange), α–SMA (green), cell nuclei (DAPI/blue). (n = 3). Bar = 50 μm. C: mRNA expression of α-SMA, D: Osteocalcin, E: Osteopontin, F: Runx2. G: Calcium content. Data is depicted as mean ± SD fold change, *p < 0.05.

In addition, both α-SMA and CD31 co-expressed with osteocalcin, indicating a potential role for EndMT in human calcific aortic valve disease. Further, α-SMA was not observed in the endothelium of a non-calcified human aortic valve leaflets. To further evaluate the *in vivo* relevance of EndMT in CAVD we assessed α-SMA expression in the aortic valve of wild type and *Apoe* $^{-/-}$ mice, a common mouse model of cardiovascular calcification [33]. Increased expression of a-SMA was observed in the endothelium of the *Apoe* $^{-/-}$ mice.

4. Discussion

We report that VICs can inhibit EndMT of VECs even when stimulated with TGF-β_1, a well-established inducer of EndMT [12,13,19,28]. We have also demonstrated that VEC osteogenic differentiation is inhibited by VICs when cultured in an osteogenic environment. Conversely, in our study, VECs did not inhibit VIC mineralization. In addition, we have shown that EndMT may precede VEC osteogenesis. Finally, EndMT was observed to co-express with osteogenic markers in a mouse model of aortic valve calcification and human aortic valves obtained from patients with calcific aortic valve disease. We thus propose that VECs contain the capacity to differentiate into endothelial-derived VICs (eVICs) through an EndMT process. In certain disease conditions where communication between VICs and VECs is disrupted, EndMT may be promoted. EndMT-derived eVICs may populate the valve leaflet and differentiate into osteoblastic cells (oVICs), contributing to the pathological remodeling observed in CAVD (Fig. 6).

This study builds on our previous work, in which we demonstrated that VEC clones from ovine mitral valve leaflets might be a source for osteoblastic VICs [14]. Endothelial osteoblastic differentiation potential has been proposed in VECs [14], prostate tumor EC [29], mutant ECs with constitutively active ALK2 [30] and in arterial endothelial cells in matrix Gla protein-deficient mice [31]. We previously showed that the *in vitro* osteogenic differentiation potential of mitral VEC corresponded with focal regions of osteogenic endothelium in tethered mitral valves *in vivo* [20]. The role of the endothelium in valve calcification was also suggested by the finding that the endothelial activation marker VCAM-1 expression correlated with VIC osteoblastic differentiation in a model of aortic valve stenosis [32]. This work also underscores the unique plasticity within subsets of VECs, which is reflected not only in diseased states but also in normal valve physiology, as evident by the co-expression of CD31 and α-SMA in human fetal and postnatal semilunar valves [19].

These findings have prompted our hypothesis that — when needed — a progenitor-like subset of VECs can replenish the VIC population via EndMT [14]. In turn, this transdifferentiation could contribute to maintaining structural integrity and function of the heart valve (Fig. 6). In normal valves, qVICs are activated by environmental cues and can differentiate into myofibroblast-like VICs

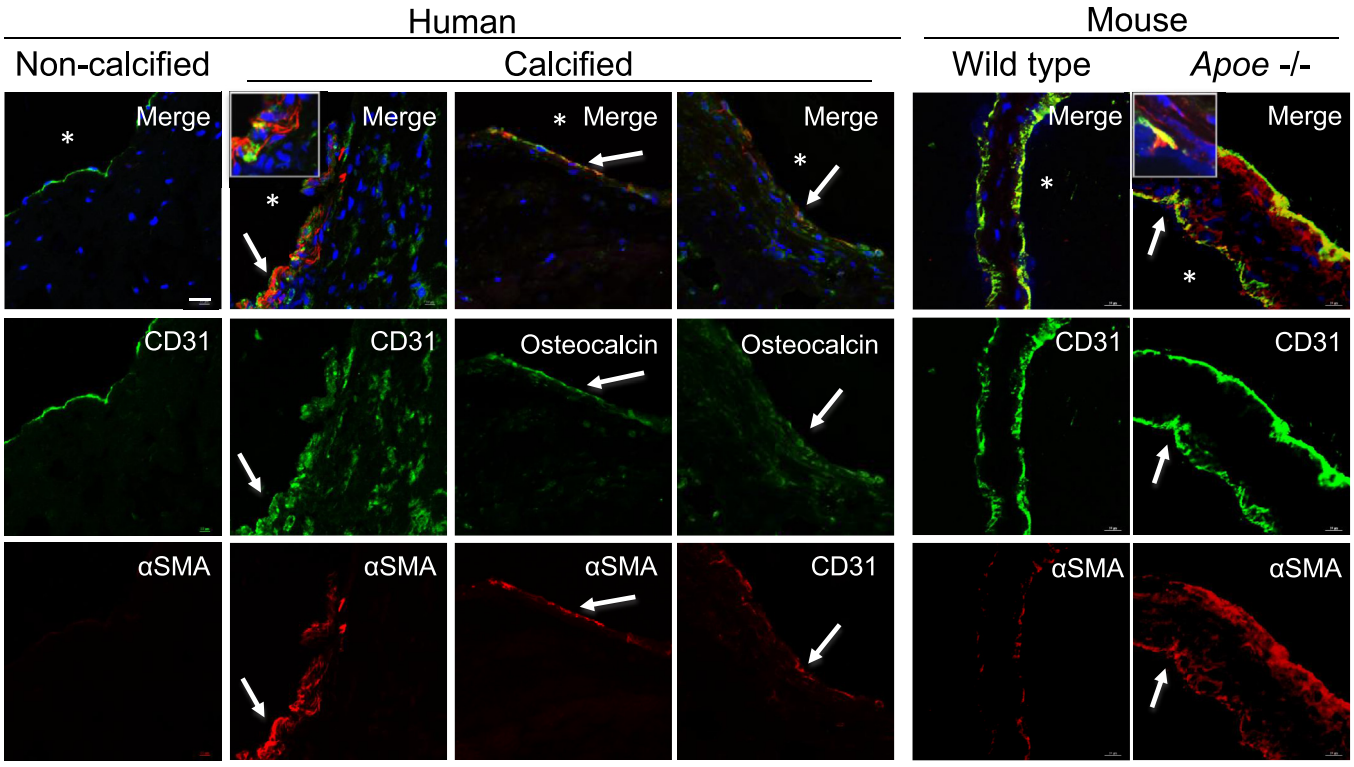

Fig. 5. Human and mouse aortic valves demonstrate EndMT. Human non-calcified and calcified aortic valves (n = 6) stained for CD31, α-SMA and osteocalcin. Aortic root sections from wild type (n = 2) and *apoE* $^{-/-}$ mice (n = 3) stained with CD31 and α-SMA. Representative images of the leaflets are shown. * Aortic side. Bar = 20 μm.

(aVICs; α-SMA-positive), which maintain tissue integrity by adaptive remodeling of the valve ECM through the secretion of various cytokines [33,34], matrix metalloproteinases [35,36], and deposition of ECM proteins [34,37]. But when persistent activation of VICs occurs, an excessive, lasting remodeling of the valve ECM may also take place. Such a maladaptive process may lead to a pathological disruption of the valve's normal connective tissue homeostasis, leading to fibrosis and eventual calcification by differentiation of oVICs [38]. Although the role of VECs in CAVD remains to be elucidated, mounting evidence indicates that endothelial dysfunction correlates with such continuous maladaptive VIC activation [38]. To our knowledge, the present work is the first to investigate VEC–VIC direct interaction in relation to osteogenesis in an *in vitro* culture model system. VICs in culture mostly demonstrate a myofibroblast-like phenotype attributed to the unnatural stiff substrate of the tissue culture plates [39]. To what extent qVICs affect VEC phenotype in co-culture remains to be elucidated. In the current experimental setup, we cannot separate the culture

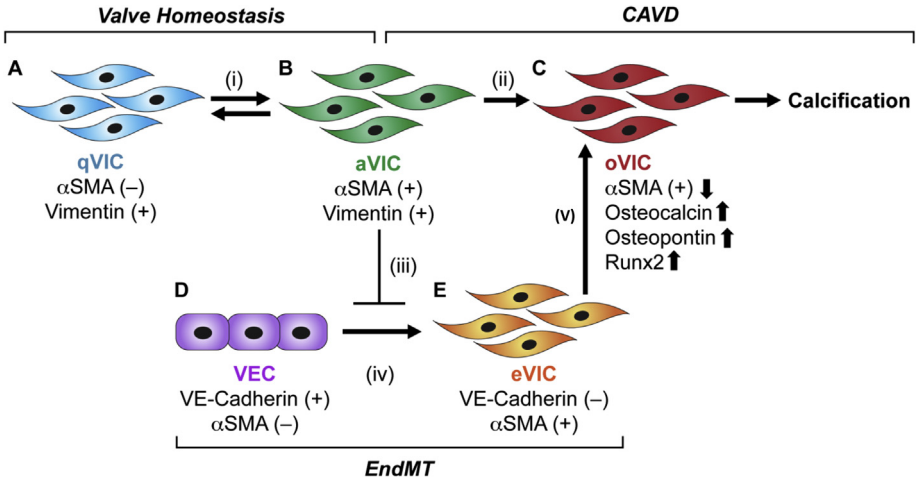

Fig. 6. Schematic depiction of cellular mechanism of the role of VECs in valvular osteogenesis. (i) Quiescent VICs (qVICs) differentiate into activated myofibroblast-like VICs (aVICs), responsible for functional remodeling of the heart valve ECM. The interplay between qVICs and aVICs is thought to be the cornerstone of valve homeostasis. (ii) Upon pathological stimulation, aVICs can further differentiate into osteoblastic VICs (oVICs), which responsible for calcium deposition in CAVD. (iii) VICs inhibit VEC EndMT. (iv) When VEC–VIC interactions are disrupted as CAVD progresses, VECs can differentiate into endothelial-derived VICs (eVICs) via EndMT. (v) eVICs may also differentiate into oVICs and contribute to calcification of the valve.

conditions to modulate VIC and VEC phenotypes independently. Therefore, both VICs and VECs were cultured in an osteogenic environment. This may be similar to the tissue, wherein both cell types are likely exposed to pathologic stimuli simultaneously, but it is possible that certain cues lead to phenotypic changes in only one cell type (e.g., hemodynamic changes that affect VECs only). Future studies may try to build on the current work to isolate changes in each cell type.

It remains unclear how closely the EndMT we have observed in VECs *in vitro* reflects the EndMT that occurs *in vivo*, either during valve development or disease. As such, it is important to note that although we demonstrate a correlation of EndMT and osteogenesis, our *in vivo* results cannot offer a causal role for VEC EndMT in CAVD. Our *in vivo* knowledge of valve EndMT mostly stems from end-point analyses of human postnatal pulmonary valve specimens or studies of the murine endocardial cushion [19], where hallmarks of EndMT consist of a loss of cell–cell contact in the EC monolayer; increased expression of α-SMA, MMP-2, and Slug; and increased cellular invasion. The present study confirms that EndMT — as determined by these hallmarks — can be simulated *in vitro*. [12] Therefore, our current results build upon previous work suggesting that EndMT plays an important role in the onset of CAVD. Aortic VECs represent a cell population with the intrinsic plasticity to differentiate into myofibroblast-like aVICs, and further into osteoblast-like oVICs. That both phenotypes have been shown to possess the potential to contribute to the development of CAVD underscores the importance of understanding the role of the valvular endothelium in the disease process. Future studies may use cell lineage tracing and cell fate models to determine the source of cells that populate the aortic valve leaflet during tissue remodeling and pathogenesis [40]. By building a better understanding the cellular contributions to the dynamic valve remodeling, specific populations of cells may be targeted to control valvular homeostasis and develop therapeutics for CAVD.

Sources of funding

This study was supported by grants from the Netherlands Heart Foundation (NHS-2011T024), Netherlands Scientific Council (NWO) to J.H., the Tommy Kaplan Discretionary Fund to J.E.M., and National Institutes of Health R01HL114805, to E.A.; and R01HL109506, to E.A. and J.B.

Disclosures

None.

Acknowledgments

The authors would like to thank Sara Karwacki for excellent editorial assistance.

Appendix A. Supplementary data

Supplementary data related to this article can be found at http://dx.doi.org/10.1016/j.atherosclerosis.2015.07.008.

References

[1] B.F. Stewart, D. Siscovick, B.K. Lind, J.M. Gardin, J.S. Gottdiener, V.E. Smith, D.W. Kitzman, C.M. Otto, Clinical factors associated with calcific aortic valve disease. Cardiovascular health study, J. Am. Coll. Cardiol. 29 (1997) 630–634.
[2] J.J. Takkenberg, N.M. Rajamannan, R. Rosenhek, A.S. Kumar, J.R. Carapetis, M.H. Yacoub, The need for a global perspective on heart valve disease epidemiology. The shvd working group on epidemiology of heart valve disease founding statement, J. Heart Valve Dis. 17 (2008) 135–139.
[3] N.M. Rajamannan, F.J. Evans, E. Aikawa, K.J. Grande-Allen, L.L. Demer, D.D. Heistad, C.A. Simmons, K.S. Masters, P. Mathieu, K.D. O'Brien, F.J. Schoen, D.A. Towler, A.P. Yoganathan, C.M. Otto, Calcific aortic valve disease: not simply a degenerative process: a review and agenda for research from the national heart and lung and blood institute aortic stenosis working group. Executive summary: calcific aortic valve disease-2011 update, Circulation 124 (2011) 1783–1791.
[4] C.M. Otto, Calcific aortic stenosis–time to look more closely at the valve, N. Engl. J. Med. 359 (2008) 1395–1398.
[5] A.C. Liu, V.R. Joag, A.I. Gotlieb, The emerging role of valve interstitial cell phenotypes in regulating heart valve pathobiology, Am. J. Pathol. 171 (2007) 1407–1418.
[6] C.M. Otto, J. Kuusisto, D.D. Reichenbach, A.M. Gown, K.D. O'Brien, Characterization of the early lesion of 'degenerative' valvular aortic stenosis. Histological and immunohistochemical studies, Circulation 90 (1994) 844–853.
[7] E.R. Mohler 3rd, F. Gannon, C. Reynolds, R. Zimmerman, M.G. Keane, F.S. Kaplan, Bone formation and inflammation in cardiac valves, Circulation 103 (2001) 1522–1528.
[8] E. Aikawa, P. Whittaker, M. Farber, K. Mendelson, R.F. Padera, M. Aikawa, F.J. Schoen, Human semilunar cardiac valve remodeling by activated cells from fetus to adult: implications for postnatal adaptation, pathology, and tissue engineering, Circulation 113 (2006) 1344–1352.
[9] J.D. Peacock, A.K. Levay, D.B. Gillaspie, G. Tao, J. Lincoln, Reduced sox9 function promotes heart valve calcification phenotypes in vivo, Circ. Res. 106 (2010) 712–719.
[10] L. Osman, M.H. Yacoub, N. Latif, M. Amrani, A.H. Chester, Role of human valve interstitial cells in valve calcification and their response to atorvastatin, Circulation 114 (2006) I547–I552.
[11] N.M. Rajamannan, M. Subramaniam, D. Rickard, S.R. Stock, J. Donovan, M. Springett, T. Orszulak, D.A. Fullerton, A.J. Tajik, R.O. Bonow, T. Spelsberg, Human aortic valve calcification is associated with an osteoblast phenotype, Circulation 107 (2003) 2181–2184.
[12] G. Paranya, S. Vineberg, E. Dvorin, S. Kaushal, S.J. Roth, E. Rabkin, F.J. Schoen, J. Bischoff, Aortic valve endothelial cells undergo transforming growth factor-beta-mediated and non-transforming growth factor-beta-mediated transdifferentiation in vitro, Am. J. Pathol. 159 (2001) 1335–1343.
[13] E.J. Armstrong, J. Bischoff, Heart valve development: endothelial cell signaling and differentiation, Circ. Res. 95 (2004) 459–470.
[14] J. Wylie-Sears, E. Aikawa, R.A. Levine, J.H. Yang, J. Bischoff, Mitral valve endothelial cells with osteogenic differentiation potential, Arterioscler. Thromb. Vasc. Biol. 31 (2011) 598–607.
[15] J.A. Madri, B.M. Pratt, A.M. Tucker, Phenotypic modulation of endothelial cells by transforming growth factor-beta depends upon the composition and organization of the extracellular matrix, J. Cell Biol. 106 (1988) 1375–1384.
[16] M.D. Combs, K.E. Yutzey, Heart valve development: regulatory networks in development and disease, Circ. Res. 105 (2009) 408–421.
[17] A.D. Person, S.E. Klewer, R.B. Runyan, Cell biology of cardiac cushion development, Int. Rev. Cytol. 243 (2005) 287–335.
[18] M.G. Frid, V.A. Kale, K.R. Stenmark, Mature vascular endothelium can give rise to smooth muscle cells via endothelial-mesenchymal transdifferentiation: in vitro analysis, Circ. Res. 90 (2002) 1189–1196.
[19] S. Paruchuri, J.H. Yang, E. Aikawa, J.M. Melero-Martin, Z.A. Khan, S. Loukogeorgakis, F.J. Schoen, J. Bischoff, Human pulmonary valve progenitor cells exhibit endothelial/mesenchymal plasticity in response to vascular endothelial growth factor-a and transforming growth factor-beta2, Circ. Res. 99 (2006) 861–869.
[20] J.P. Dal-Bianco, E. Aikawa, J. Bischoff, J.L. Guerrero, M.D. Handschumacher, S. Sullivan, B. Johnson, J.S. Titus, Y. Iwamoto, J. Wylie-Sears, R.A. Levine, A. Carpentier, Active adaptation of the tethered mitral valve: insights into a compensatory mechanism for functional mitral regurgitation, Circulation 120 (2009) 334–342.
[21] M. Chaput, M.D. Handschumacher, J.L. Guerrero, G. Holmvang, J.P. Dal-Bianco, S. Sullivan, G.J. Vlahakes, J. Hung, R.A. Levine, M.T.N. Leducq Foundation, Mitral leaflet adaptation to ventricular remodeling: prospective changes in a model of ischemic mitral regurgitation, Circulation 120 (2009) S99–S103.
[22] K. Balachandran, P.W. Alford, J. Wylie-Sears, J.A. Goss, A. Grosberg, J. Bischoff, E. Aikawa, R.A. Levine, K.K. Parker, Cyclic strain induces dual-mode endothelial-mesenchymal transformation of the cardiac valve, Proc. Natl. Acad. Sci. U. S. A. 108 (2011) 19943–19948.
[23] D. Skowasch, S. Schrempf, N. Wernert, M. Steinmetz, A. Jabs, I. Tuleta, U. Welsch, C.J. Preusse, J.A. Likungu, A. Welz, B. Luderitz, G. Bauriedel, Cells of primarily extra-valvular origin in degenerative aortic valves and bioprostheses, Eur. Heart J. 26 (2005) 2576–2580.
[24] K. Bosse, C.P. Hans, N. Zhao, S.N. Koenig, N. Huang, A. Guggilam, S. LaHaye, G. Tao, P.A. Lucchesi, J. Lincoln, B. Lilly, V. Garg, Endothelial nitric oxide signaling regulates notch1 in aortic valve disease, J. Mol. Cell. Cardiol. 60 (2013) 27–35.
[25] J. Richards, I. El-Hamamsy, S. Chen, Z. Sarang, P. Sarathchandra, M.H. Yacoub, A.H. Chester, J.T. Butcher, Side-specific endothelial-dependent regulation of aortic valve calcification: interplay of hemodynamics and nitric oxide signaling, Am. J. Pathol. 182 (2013) 1922–1931.
[26] J.M. Melero-Martin, M.E. De Obaldia, S.Y. Kang, Z.A. Khan, L. Yuan, P. Oettgen, J. Bischoff, Engineering robust and functional vascular networks in vivo with human adult and cord blood-derived progenitor cells, Circ. Res. 103 (2008) 194–202.

[27] J.H. Yang, J. Wylie-Sears, J. Bischoff, Opposing actions of Notch1 and VEGF in post-natal cardiac valve endothelial cells, Biochem. Biophys. Res. Commun. 374 (2008) 512–516.
[28] E.L. Dvorin, J. Jacobson, S.J. Roth, J. Bischoff, Human pulmonary valve endothelial cells express functional adhesion molecules for leukocytes, J. Heart Valve Dis. 12 (2003) 617–624.
[29] A.C. Dudley, Z.A. Khan, S.C. Shih, S.Y. Kang, B.M. Zwaans, J. Bischoff, M. Klagsbrun, Calcification of multipotent prostate tumor endothelium, Cancer Cell 14 (2008) 201–211.
[30] D. Medici, E.M. Shore, V.Y. Lounev, F.S. Kaplan, R. Kalluri, B.R. Olsen, Conversion of vascular endothelial cells into multipotent stem-like cells, Nat. Med. 16 (2010) 1400–1406.
[31] Y. Yao, M. Jumabay, A. Ly, M. Radparvar, M.R. Cubberly, K.I. Bostrom, A role for the endothelium in vascular calcification, Circ. Res. 113 (2013) 495–504.
[32] E. Aikawa, M. Nahrendorf, D. Sosnovik, V.M. Lok, F.A. Jaffer, M. Aikawa, R. Weissleder, Multimodality molecular imaging identifies proteolytic and osteogenic activities in early aortic valve disease, Circulation 115 (2007) 377–386.
[33] A.H. Chester, P.M. Taylor, Molecular and functional characteristics of heart-valve interstitial cells, Philos. Trans. R. Soc. Lond. Ser. B Biol. Sci. 362 (2007) 1437–1443.
[34] G.A. Walker, K.S. Masters, D.N. Shah, K.S. Anseth, L.A. Leinwand, Valvular myofibroblast activation by transforming growth factor-beta: implications for pathological extracellular matrix remodeling in heart valve disease, Circ. Res. 95 (2004) 253–260.
[35] E. Rabkin, M. Aikawa, J.R. Stone, Y. Fukumoto, P. Libby, F.J. Schoen, Activated interstitial myofibroblasts express catabolic enzymes and mediate matrix remodeling in myxomatous heart valves, Circulation 104 (2001) 2525–2532.
[36] E. Rabkin-Aikawa, M. Farber, M. Aikawa, F.J. Schoen, Dynamic and reversible changes of interstitial cell phenotype during remodeling of cardiac valves, J. Heart Valve Dis. 13 (2004) 841–847.
[37] M.C. Cushing, J.T. Liao, K.S. Anseth, Activation of valvular interstitial cells is mediated by transforming growth factor-beta1 interactions with matrix molecules, Matrix Biol. J. Int. Soc. Matrix Biol. 24 (2005) 428–437.
[38] R.B. Hinton Jr., J. Lincoln, G.H. Deutsch, H. Osinska, P.B. Manning, D.W. Benson, K.E. Yutzey, Extracellular matrix remodeling and organization in developing and diseased aortic valves, Circ. Res. 98 (2006) 1431–1438.
[39] H. Wang, M.W. Tibbitt, S.J. Langer, L.A. Leinwand, K.S. Anseth, Hydrogels preserve native phenotypes of valvular fibroblasts through an elasticity-regulated pi3k/akt pathway, Proc. Natl. Acad. Sci. U. S. A. 110 (2013) 19336–19341.
[40] R.P. Visconti, Y. Ebihara, A.C. LaRue, P.A. Fleming, T.C. McQuinn, M. Masuya, H. Minamiguchi, R.R. Markwald, M. Ogawa, C.J. Drake, An in vivo analysis of hematopoietic stem cell potential: hematopoietic origin of cardiac valve interstitial cells, Circ. Res. 98 (2006) 690–696.